Pinch current limitation effect in plasma focus

S. Lee[a)]
Nanyang Technological University, National Institute of Education, Singapore 637616 and INTI International University College, 71800 Nilai, Malaysia

S. H. Saw
INTI International University College, 71800 Nilai, Malaysia

(Received 8 November 2007; accepted 3 December 2007; published online 17 January 2008)

The Lee model couples the electrical circuit with plasma focus dynamics, thermodynamics, and radiation. It is used to design and simulate experiments. A beam-target mechanism is incorporated, resulting in realistic neutron yield scaling with pinch current and increasing its versatility for investigating all Mather-type machines. Recent runs indicate a previously unsuspected "pinch current limitation" effect. The pinch current does not increase beyond a certain value however low the static inductance is reduced to. The results indicate that decreasing the present static inductance of the PF1000 machine will neither increase the pinch current nor the neutron yield, contrary to expectations. © *2008 American Institute of Physics*. [DOI: 10.1063/1.2827579]

This model in its two-phase form was described in 1984.[1] It was used to assist in the design and interpretation of several experiments.[2–4] An improved five-phase model and code incorporating finite small disturbance speed,[5] radiation and radiation coupling with dynamics assisted several projects,[6–8] and was web published[9] in 2000 and in 2005.[10] Plasma self-absorption was included[9] in 2007. It has been used extensively as a complementary facility in several machines, for example, UNU/ICTP PFF,[2,6] the NX2,[7,8] NX1,[7] and DENA.[11] It has also been used[12] in other machines for design and interpretation including Soto's subkilojoule plasma focus machines,[13] FNII,[14] and the UBA hard x-ray source.[15] Information obtained from the model includes axial and radial velocities and dynamics,[1,7,12,11] soft x-ray (SXR) emission characteristics and yield,[5,7,8,16] design of machines,[13,16] optimization of machines, and adaptation to other machine types such as the Filippov-type DENA.[11] A study of speed-enhanced neutron yield[4,13] was also assisted by the model code.

A detailed description of the model is already available on the internet.[9,10] A recent development in the code is the inclusion of neutron yield using a phenomenological beam-target neutron generating mechanism,[17] incorporated in the present RADPFV5.13. A beam of fast deuteron ions is produced by diode action in a thin layer close to the anode, with plasma disruptions generating the necessary high voltages. The beam interacts with the hot dense plasma of the focus pinch column to produce the fusion neutrons. In this modeling, each factor contributing to the yield is estimated as a proportional quantity and the yield is obtained as an expression with proportionality constant. The yield is then calibrated against a known experimental point.

The beam-target yield is written in the form $Y_{b-t} \sim n_b n_i (r_p^2 z_p)(\sigma v_b)\tau$ where n_b is the number of beam ions per unit plasma volume, n_i is the ion density, r_p is the radius of the plasma pinch with length z_p, σ is the cross section of the D–D fusion reaction, n branch,[18] v_b is the beam ion speed, and τ is the beam-target interaction time assumed proportional to the confinement time of the plasma column.

Total beam energy is estimated[17] as proportional to $L_p I_{\text{pinch}}^2$,[2] a measure of the pinch inductance energy, L_p being the focus pinch inductance. Thus, the number of beam ions is $N_b \sim L_p I_{\text{pinch}}^2 / v_b^2$ and n_b is N_i divided by the focus pinch volume. Note that $L_p \sim \ln(b/r_p) z_p$, that[4] $\tau \sim r_p \sim z_p$, and that $v_b \sim U^{1/2}$ where U is the disruption-caused diode voltage.[17] Here, b is the cathode radius. We also assume reasonably that U is proportional to $V_{\max}$, the maximum voltage induced by the current sheet collapsing radially toward the axis.

Hence, we derive
$$Y_{b-t} = C_n I_{\text{pinch}}^2 z_p^2 [(\ln b/r_p)] \sigma / V_{\max}^{1/2}, \qquad (1)$$

where I_{pinch} is the current flowing through the pinch at start of the slow compression phase; r_p and z_p are the pinch dimensions at end of that phase. Here, C_n is a constant which, in practice, we will calibrate with an experimental point.

The D–D cross section is highly sensitive to the beam energy so it is necessary to use the appropriate range of beam energy to compute σ. The code computes $V_{\max}$ of the order of 20–50 kV. However, it is known[17] from experiments that the ion energy responsible for the beam-target neutrons is in the range of 50–150 keV,[17] and for smaller lower-voltage machines the relevant energy[19] could be lower at 30–60 keV. Thus, to align with experimental observations the D–D cross section σ is reasonably obtained by using beam energy equal to three times $V_{\max}$.

A plot of experimentally measured neutron yield Y_n vs I_{pinch} was made combining all available experimental data.[2,4,11,13,17,19–22] This gave a fit of $Y_n = 9 \times 10^{10} I_{\text{pinch}}^{3.8}$ for I_{pinch} in the range 0.1–1 MA. From this plot, a calibration point was chosen at 0.5 MA, $Y_n = 7 \times 10^9$ neutrons. The model code[23] RADPFV5.13 was thus calibrated to compute Y_{b-t} which in our model is the same as Y_n.

From experience, it is known that the current trace of the focus is one of the best indicators of gross performance. The axial and radial phase dynamics and the crucial energy transfer into the focus pinch are among the important information that is quickly apparent from the current trace. Numerical experiments were carried out for machines for which reliable current traces and neutron yields are available. Figure 1 shows a comparison of the computed total current trace

[a)]Electronic mail: leesing@optusnet.com.au.

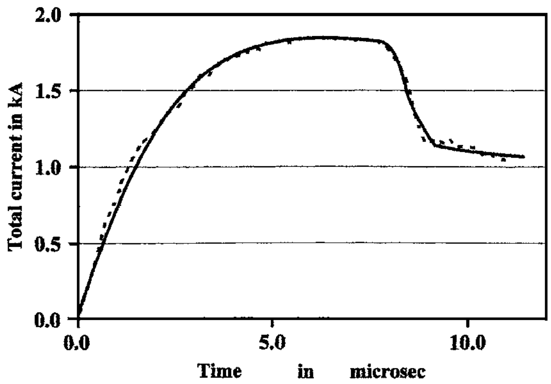

FIG. 1. PF1000 at 27 kV measured (dashed line) vs computed (smooth line) current traces.

(solid smooth line) with the experimental trace (dotted line) of the PF1000 at 27 kV (Ref. 17), 3.5 torr deuterium, with outer/inner radii b=16 cm, a=11.55 cm, and anode length z_o=60 cm. In the numerical experiments we fitted external (or static) inductance L_o=33 nH and stray resistance r_o=6 mΩ with model parameters mass factor, current factor, and radial mass factor as f_m=0.14, f_c=0.7, and f_{mr}=0.35. The computed current trace agrees very well with the experiment, a typical performance of this code.

Each numerical experiment is considered satisfactory when the computed current trace matches the experiment in current rise profile and peak current, in time position of the current dip, in slope, and absolute value of the dip (see Fig. 1). The results were obtained for the PF400, the UNU/ICTP PFF, the NX2, and PF1000 at 35 kV; for which current traces and neutron yields are available. We thus established these reliable points for our computed Y_n data. To make the results less sketchy, additional points were obtained for the PF1000 from 13.5 to 40 kV though these additional points are not supported by published results. More work will need to be done. However, even with the results obtained, it is clear that the model code is producing a scaling of $Y_n \sim I_{\text{pinch}}^{4.7}$; and $Y_n \sim I_{\text{peak}}^{3.9}$. These computed scaling laws are in reasonable agreement with those put up from time to time by experimental compilations,[20,21] considering that in the experimental results, I_{pinch} is seldom properly measured, in many cases, only estimated from I_{peak}. Such estimates are dicey since the relationship between the peak total current I_{peak} (measured in the external circuit) and the pinch current I_{pinch} flowing in the tube is variable. Our code is consistent in that I_{pinch} is rigorously computed by fitting the total current trace. This gives confidence in the scaling ability of the code for Y_n as well.

An important question is how to improve the neutron yields of experiments. One obvious strategy is to increase I_{pinch} by reducing L_o. For example, the 30 μF, 110 nH UNU/ICTPPFF (Refs. 2, 4, 12, and 19) had its L_o reduced to 20 nH evolving, as it were, into the NX2.[7,16,22] I_{peak} more than doubled. More importantly, though less than doubled, I_{pinch} increased from 120 to 220 kA. Neutron yields increased three to five times, as did SXR yields.

What about a bank such as the PF1000? With C_o at 1332 μF, its L_o of 30 nH (fitted by the code) is already low relative to its huge C_o. We have run the code using the machine and model parameters determined from Fig. 1, modified by information about values of I_{peak} at 35 kV. Operating the PF1000 at 35 kV and 3.5 torr, we varied the anode radius a (with corresponding adjustment to b to maintain a constant $c=b/a$) to keep the peak axial speed at 10 cm/μs. The anode length z_o was also adjusted to maximize I_{pinch}.

L_o was decreased from 100 nH progressively to 5 nH. As expected, I_{peak} increased from 1.66 to 4.4 MA. As L_o was reduced from 100 to 35 nH, I_{pinch} also increased, from 0.96 to 1.05 MA. However, then unexpectedly on further reduction from 35 to 5 nH, I_{pinch} stopped increasing, instead decreasing slightly to 1.03 MA at 20 nH, to 1.0 MA at 10 nH, and to 0.97 MA at 5 nH. Y_n also had a maximum value of 3.2×10^{11} at 35 nH.

To explain this unexpected result, we examine the energy distribution in the system at the end of the axial phase (see Fig. 1) just before the current drops from peak value I_{peak} and then again near the bottom of the almost linear drop to I_{pinch}. The energy equation describing this current drop is written as follows:

$$0.5I_{\text{peak}}^2(L_o+L_af_c^2)=0.5I_{\text{pinch}}^2(L_o/f_c^2+L_a+L_p)+\delta_{\text{cap}}+\delta_{\text{plasma}}, \quad (2)$$

where L_a is the inductance of the tube at full axial length z_o. δ_{plasma} is the energy imparted to the plasma as the current sheet moves to the pinch position and is the integral of $0.5(dL/dt)I^2$. We approximate this as $0.5L_pI_{\text{pinch}}^2$ (which is an underestimate) for this case. δ_{cap} is the energy flow into or out of the capacitor during this period of current drop. If the duration of the radial phase is short compared to the capacitor time constant, the capacitor is effectively decoupled and δ_{cap} may be put as zero. From this consideration we obtain

$$I_{\text{pinch}}^2=I_{\text{peak}}^2(L_o+0.5L_a)/(2L_o+L_a+2L_p), \quad (3)$$

where we have taken f_c=0.7 and approximated f_c^2 as 0.5.

Taking the example of PF1000 at 35 kV we obtain for each L_o the corresponding L_a ($\sim$0.65 nH/cm of z_o) and L_p [$\sim$3.8 nH/cm of (Ref. 4) $z_p\sim a$]. For example, at L_o=100 nH, L_a=52 nH, and L_p=29 nH giving $I_{\text{pinch}}/I_{\text{peak}}$ as 0.63. This ratio drops progressively as L_o decreases. For L_o=5 nH, L_a=13 nH, and L_p=77 nH giving the ratio as 0.25. The results show that as L_o is reduced from 100 nH, at first, the increase in I_{peak} more than compensates for the drop in $I_{\text{pinch}}/I_{\text{peak}}$ and I_{pinch} increases from L_o=100 nH to L_o=40 nH. Below L_o=40 nH, the drop in $I_{\text{pinch}}/I_{\text{peak}}$ catches up with the increase in I_{peak} leading to the numerically observed flat maximum of I_{pinch}. Y_n also has a flat maximum of 3.2×10^{11} at L_o=40–30 nH.

The current limitation can now be seen as firstly a consequence of Eq. (3). Generally, as L_o is reduced, I_{peak} increases; a is necessarily increased leading (Ref. 4) to a longer pinch length z_p, hence a bigger L_p. Lowering L_o also results in a shorter rise time, hence a necessary decrease in z_o, reducing L_a. Thus, from Eq. (3), lowering L_o decreases the fraction $I_{\text{pinch}}/I_{\text{peak}}$. Secondly, this situation is compounded by another mechanism. As L_o is reduced, the L-C interaction time of the capacitor bank reduces while the duration of the current drop increases due to an increasing a. This means that as L_o is reduced, the capacitor bank is more and more coupled to the inductive energy transfer processes with the accompanying induced large voltages that arise from the radial compression. Looking again at the derivation of Eq. (3) from Eq. (2) a nonzero δ_{cap}, in this case, of positive value, will act to decrease I_{pinch} further. The lower L_o the more pronounced is this effect.

Summarizing this discussion, the pinch current limitation is not a simple effect, but is a combination of the two complex effects described above, namely, the interplay of the various inductances involved in the plasma focus processes abetted by the increasing coupling of C_o to the inductive energetic processes, as L_o is reduced.

We carried out several sets of experiments on the PF1000, each set with a different damping factor. In every case, an optimum inductance was found around 30–60 nH with I_{pinch} decreasing as L_o was reduced below the optimum value. We also carried out another set of experiments with a planned focus with C_o of 300 μF. For that device, optimum L_o was found to be 20 nH. More sets of experiments need to be run to gain further experience and insight to understand better the complex interactions of the several parameters that conspire to determine the optimum L_o. The results of these ongoing studies will be published in more detail in due course.

In the meantime, enough information has been obtained from the numerical experiments to enable a statement that for PF1000, reducing L_o from its present 20–30 nH will increase neither the observed I_{pinch}, nor the neutron yield.

The prevailing thinking seems to be that the lower L_o is made, the higher performance a plasma focus would have in terms of driving current and Y_n. This paper shows that, on the contrary, given a fixed C_o powering a plasma focus, there exists an optimum L_o for maximum I_{pinch}. Reducing L_o further will increase neither I_{pinch} nor Y_n. Plasma focus research now has to meet the challenges posed by this "pinch current limitation" effect.

[1]S. Lee in *Laser and Plasma Technology*, edited by S. Lee, B. C. Tan, C. S. Wong, and A. C. Chew (World Scientific, Singapore, 1985), pp. 387–420.

[2]S. Lee, T. Y. Tou, S. P. Moo, M. A. Elissa, A. V. Gholap, K. H. Kwek, S. Mulyodrono, A. J. Smith, Suryadi, W. Usala, and M. Zakaullah, Am. J. Phys. **56**, 62 (1988).

[3]T. Y. Tou, S. Lee, and K. H. Kwek, IEEE Trans. Plasma Sci. **17**, 311 (1989).

[4]S. Lee and A. Serban, IEEE Trans. Plasma Sci. **24**, 1101 (1996).

[5]D. E. Potter, Phys. Fluids **14**, 1911 (1971).

[6]M. H. Liu, X. P. Feng, S. V. Springham, and S. Lee, IEEE Trans. Plasma Sci. **26**, 135 (1998).

[7]S. Lee, P. Lee, G. Zhang, X. Feng, V. A. Gribkov, M. Liu, A. Serban, and T. Wong, IEEE Trans. Plasma Sci. **26**, 1119 (1998).

[8]S. Bing, "Plasma dynamics and x-ray emission of the plasma focus," Ph.D. thesis, NIE, 2000 (in ICTP Open Access Archive: http://eprints.ictp.it/99/)

[9]S. Lee, in http://ckplee.myplace.nie.edu.sg/plasmaphysics/ (2000 and 2007).

[10]S. Lee in ICTP Open Access Archive: http://eprints.ictp.it/85/ (2005).

[11]V. Siahpoush, M. A. Tafreshi, S. Sobhanian, and S. Khorram, Plasma Phys. Controlled Fusion **47**, 1065 (2005).

[12]S. Lee, Twelve Years of UNU/ICTP PFF-A Review (1998) IC, 98 (231); A. Salam ICTP, Miramare, Trieste (in ICTP OAA: http://eprints.ictp.it/31/).

[13]L. Soto, P. Silva, J. Moreno, G. Silvester, M. Zambra, C. Pavez, L. Altamirano, H. Bruzzone, M. Barbaglia, Y. Sidelnikov, and W. Kies, Braz. J. Phys. **34**, 1814 (2004).

[14]H. Acuna, F. Castillo, J. Herrera, and A. Postal, International Conference on Plasma Sci, 3–5 June 1996 (unpublished), p. 127.

[15]C. Moreno, V. Raspa, L. Sigaut, and R. Vieytes, Appl. Phys. Lett. **89**, 15 (2006).

[16]D. Wong, P. Lee, T. Zhang, A. Patran, T. L. Tan, R. S. Rawat, and S. Lee, Plasma Sources Sci. Technol. **16**, 116 (2007).

[17]V. A. Gribkov, A. Banaszak, B. Bienkowska, A. V. Dubrovsky, I. Ivanova-Stanik, L. Jakubowski, L. Karpinski, R. A. Miklaszewski, M. Paduch, M. J. Sadowski, M. Scholz, A. Szydlowski, and K. Tomaszewski, J. Phys. D **40**, 3592 (2007).

[18]J. D. Huba, 2006 Plasma Formulary, p. 44. http://wwwppd.nrl.navy.mil/nrlformulary/NRL_FORMULARY_07.pdf

[19]S. V. Springham, S. Lee, and M. S. Rafique, Plasma Phys. Controlled Fusion **42**, 1023 (2000).

[20]W. Kies, in *Laser and Plasma Technology*, Proceedings of Second Tropical College, edited by S. Lee, B. C. Tan, C. S. Wong, A. C. Chew, K. S. Low, H. Ahmad, and Y. H. Chen (World Scientific, Singapore, 1988), pp. 86–137.

[21]H. Herold, in *Laser and Plasma Technology*, Proceedings of Third Tropical College, edited by C. S. Wong, S. Lee, B. C. Tan, A. C. Chew, K. S. Low, and S. P. Moo (World Scientific, Singapore, 1990), pp. 21–45.

[22]A. Patran, R. S. Rawat, J. M. Koh, S. V. Springham, T. L. Tan, P. Lee, and S. Lee, 31st EPS Conference on Plasma Physics London, 2004 (unpublished), Vol. 286, p. 4.213.

[23]http://www.intimal.edu.my/school/fas/UFLF/

Erratum

The published paper contains 2 errors on page 1 which are corrected by this note. The relevant paragraph is reproduced here in parenthesis with the corrections highlighted in bold red:

"Total beam energy is estimated[17] as proportional to $L_p I_{pinch}^2$, a measure of the pinch inductance energy, L_p being the focus pinch inductance. Thus the number of beam ions is $N_b \sim L_p I_{pinch}^2 / v_b^2$ and n_b is **N_b** divided by the focus pinch volume. Note that $L_p \sim \ln(b/r_p) z_p$, that[4] $\tau \sim r_p \sim z_p$, and that $v_b \sim U^{1/2}$ where U is the disruption-caused diode voltage[17]. Here 'b' is the cathode radius. We also assume reasonably that U is proportional to V_{max}, the maximum voltage induced by the current sheet collapsing radially towards the axis.

Hence we derive: $$Y_{b\text{-}t} = C_n \, \mathbf{n_i} \, I_{pinch}^2 z_p^2 ((\ln b/r_p))\sigma / V_{max}^{1/2} \quad (1)$$

where I_{pinch} is the current flowing through the pinch at start of the slow compression phase; r_p and z_p are the pinch dimensions at end of that phase. Here C_n is a constant which in practice we will calibrate with an experimental point."

There is another error on page 2, Fig 1. The vertical axis should be labeled 'Total Current in MA'.